Chapter

Effect of Molecular Structure Modification and Nano-Doping on Charge Transportation of Polyimide Films for Winding Insulation

Boxue Du, Ranran Xu, Jiwen Xing and Jin Li

Abstract

Polyimide (PI) is widely employed as winding insulation in high voltage devices, such as extra-high voltage electric reactor and inverter-fed motor. The injection and accumulation of charges on the surface of PI films will lead to electrical field distortion and reduced lifespan of winding insulation, especially for the operation environment of high temperature and high voltage. This chapter focuses on effects of surface molecular modification and nanoparticles on dynamic characteristics of surface charge and space charge of pure PI films, including three sections. The effect of molecular structure on the surface charge dynamics of PI films was studied firstly. The chapter investigated that how molecular structure affects surface charge of polyimide nanocomposite films. Furthermore, the effect of surface molecular modification on space charge characteristics of multilayer PI films was researched. The results illustrate that surface molecular modification and nanoparticles can comprehensively suppress space charge accumulation and improve dielectric property.

Keywords: polyimide, surface molecular modification, nanoparticles, surface charge, space charge

1. Introduction

Polyimide film (PI) is widely applied in reactor extra-high voltage (EHV) winding insulation, wind turbine winding, and variable frequency motor winding insulation due to its excellent physical, chemical, and heat resistance properties, with the wide range of applications in electronics and aerospace. During the operation of electrical equipment, the corona and partial discharge will inevitably happen and be accompanied by temperature rise [1], making insulation materials of EHV equipment in a complex environment where high temperature, high voltage, corona, and partial discharge exist together for a long time. A large amount of surface and space charge will inject into insulation materials, leading to the accumulation of local charges in the insulation and electrical field distortion, which will reduce the life of

equipment. Therefore, it is vital to study the surface charge and space charge transport mechanism of polyimide to improve the electrical properties of the film.

Nanocomposite dielectrics have shown excellent insulation performance due to the special size effect of nanoparticles, especially in corona resistance. Plenty of researchers have added inorganic nanoparticles to the polymer matrix to prepare nanocomposite dielectrics and achieved some results in practical applications [2–8]. Zhong added the silane coupling agent when preparing the SiO_2/PI composite films, the results showed that the coupling agent improved the dispersion of the nanoparticles and the interface morphology [9]. Zha Junwei et al. prepared PI/ZnO composite films via in-situ polymerization, with studying the material's electrical resistance, volume resistivity, dielectric constant, and dielectric loss, the better corona resistance of the composite films is acquired. However, both the dielectric loss and the dielectric constant increase with the growth of the ZnO content [10]. The Al_2O_3/PI composite films were prepared using in-situ polymerization. The corona resistance testing results showed that the corona resistance improved when the mass fraction of nano-Al_2O_3 increased, and the corona resistance reaches the peak when in 20 wt%. Nevertheless, the agglomeration phenomenon becomes more and more obvious with the mass fraction gradually starts from 5 wt%, observed by the electron microscope [11]. Based on the above studies, it can be found that some achievements have been obtained in the nano-doped polyimide films, but its electrical resistance is not ideal. The research status of nano-composite polyimide films is still lingering in pursuing higher content of inorganic nanoparticles, better compatibility, and the better physical and chemical structure of nanocomposites. The surface and space charges have not been studied.

On the other hand, the electrical properties of fluoropolymers have not attracted the attention of researchers. In fact, the molecular structure modification (fluorination), as a kind of polymer surface chemical structure that changes the chemical composition of the polymer surface layer, has mature applications in the chemical industry [12, 13]. A Zhenlian found that the fluorocarbon layer is formed on the surface of polyethylene by fluorination, and the space charge characteristics have been studied [14]. It was found that the fluorinated layer can suppress the space charge injection. However, the current research has not carried out on the dynamic characteristics of surface and space charge accumulation as well as dissipation and on the effect of the introduction of fluorine on the depth of dielectric traps. So far, the application of surface fluorination is mainly used to improve the adhesion properties, barrier properties, and anti-permeability properties of polymers. There are few reports on its application in electrical insulation [15]. In the chapter, the molecular structure modification is used to control the surface structure of polyimide film and nano-composite polyimide film, and the surface and space charge dynamic characteristics of the film are studied to develop new polymer dielectrics, which is important in the field of engineering dielectric.

2. Experiments

2.1 The sample preparation

The chapter uses the two-step method to prepare the polyimide films. Pyromellitic dianhydride (PMDA) and 4,4′-diaminodiphenyl ether (ODA) are added into dimethylacetamide (DMAc). The polyamic acid (PAA) was prepared by polymerization reaction in the process. The PAA was coated on the glass plate, placed in a vacuum environment to remove air inside PAA, which was placed in the environment where the temperature was 60°C (1 h), 120°C (2 h), 150°C (1 h),

200°C (1 h), 250°C (1 h) and 300°C (1 h). After the heating was stopped, waited for 6 hours, and the PI film with a certain thickness was prepared.

In addition, the nano-composite polyimide film was prepared by in-situ polymerization. Firstly, the nano-particles Al_2O_3 (particle size is less than 20 nm) and surface modifier KH550 were placed in an organic solvent DMAc for ultrasonic process for 1 hour to ensure that the nanoparticles are uniformly dispersed in the organic solvent. Then the appropriate amount of ODA was added into solution and stir for 1 hour. The PMDA was added to the suspension in batches under the water bath environment at a constant temperature of 40°C, and mechanical stirring was continued until the viscosity of the entire reaction solution suddenly increased. After degassing and imidization, PI films doping with different contents of Al_2O_3 (0, 1, 3, 5, 7 wt%) with a certain thickness were obtained. The scanning electron microscope (SEM) was used to observe the presence of nanoparticles in distribution in the PI matrix.

The surface molecular modification is achieved in terms of surface fluorination. The PI sample is placed in a closed reactor, the air inside the reactor is purged, and the reactor is filled with a certain proportion of fluorine gas and nitrogen gas mixture (12.5 and 20%). The internal reaction temperature was adjusted by the temperature control device (reaction temperature is room temperature and 55°C, respectively), the air pressure was 500 mbar, and the reaction time was 15, 30, 45, and 60 min. The sample after surface molecular modification was used to study the effect of different reaction time on the surface and space charge of the PI sample. The SEM and infrared spectrum analysis tester were used to verify the effect of fluorination.

The multilayer PI sample is a composite of pure single-layer PI film with the same fluorination time.

2.2 Testing method

2.2.1 Surface charge dynamic characteristics experiment

The surface charge measurement system is shown in **Figure 1(a)**. The entire corona measuring device is in a closed transparent container to ensure the same temperature and humidity. The needle plate electrode was used, the plate electrode is below the needle electrode, the distance between the needle tip and the plate electrode is 5 mm, and the distance between the plate and the surface of sample is

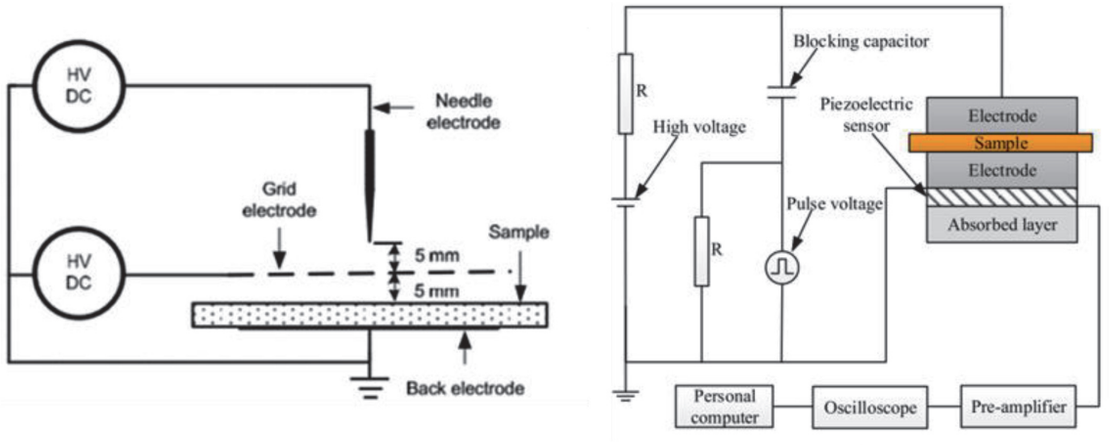

(a) (b)

Figure 1.
(a) Surface charge measurement system and (b) space charge measurement system.

also 5 mm. The sample is placed on the ground electrode. Turn on the voltage power supply, and the corona time is 10, 20, and 30 min. When the corona time is reached, turn off the high voltage power supply, quickly transfer the sample to the electrostatic potentiometer and record its surface potential for 4 hours.

According to the measured results, the surface charge density can be calculated, and the calculation formula is

$$\sigma = \frac{\varepsilon_0 \varepsilon_r}{d} V_{(t_0)} \tag{1}$$

Among them, σ is the required surface charge density, d is the thickness of the sample, V is the sample surface potential, ε_0 and ε_r are the vacuum dielectric constant and the relative dielectric constant [16].

2.2.2 Space charge dynamic characteristics experiment

This chapter uses the pulsed electro-acoustic (PEA) method to test and study the space charge dynamic distribution in the PI sample. The measurement device is shown in **Figure 1(b)**, which mainly is made up of high voltage DC power supply, pulse generator, electrode system, preamplifier, computer, and oscilloscope. The measuring principle is that a pulse voltage is applied across the sample, and this pulse will generate an electric field inside the sample, causing space charge vibration in the sample. This vibration is propagated outward by means of sound waves. The amplitude of sound waves stands for the amount of charge, and the time when the acoustic wave reaches the piezoelectric sensor reflects the position of the space charge in the sample. During the test, the applied DC voltage was 5000 V, the measuring time was 3600 s, and data were recorded per 600 s. In addition, the ambient temperature was 25°C, and the relative humidity was ~40%.

3. Results and discussion

3.1 The effect of molecular structure on the surface charge dynamics of PI films

The ATR-FTIR spectrum of the PI films before and after fluorination is shown in **Figure 2**. In **Figure 2(a)**, the infrared spectrum of the original polyimide film was described. From the graph, we can find the typical characteristics of PI films, with the absorption peaks at 1780 and 1720 cm^{-1}. Furthermore, the absorption peaks of the C═C double bond of the benzene ring are at 1500 and 1100 cm^{-1}, the vibrational absorption peaks of the C—N bond are at 1373 cm^{-1}, and the absorption peaks at 810 cm^{-1} are the vibration of benzene-H bond. The absorption peak at 1237 and 3200 cm^{-1} indicates that a small amount of ODA remained during the molecular polymerization reaction. The infrared spectrum of the sample after fluorination is shown in **Figure 2(b)**. As can be seen that the PI film after the surface molecular structure has the obvious C—F, C—F_2 and C—F_3 absorption peak is in the range of 950–1340 cm^{-1}. **Figure 2** shows that the C—F bond is the strongest bond in the polymer, higher a great than the C—H bond. So, the surface fluorination will make the fluorine element replace the hydrogen element on the PI films surface, which results in the reduction and even disappearance of C—H bonds in the molecular structure of the surface layer and accompanied by the formation of C—F, C—F_2, and C—F_3. There is a dense C—F layer on the PI film surface layer.

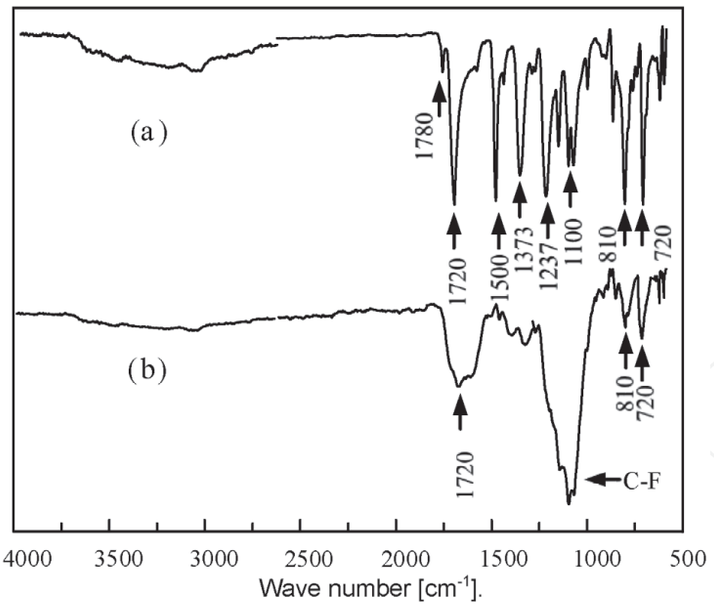

Figure 2.
The infrared spectrum of (a) original film and (b) fluorinated film.

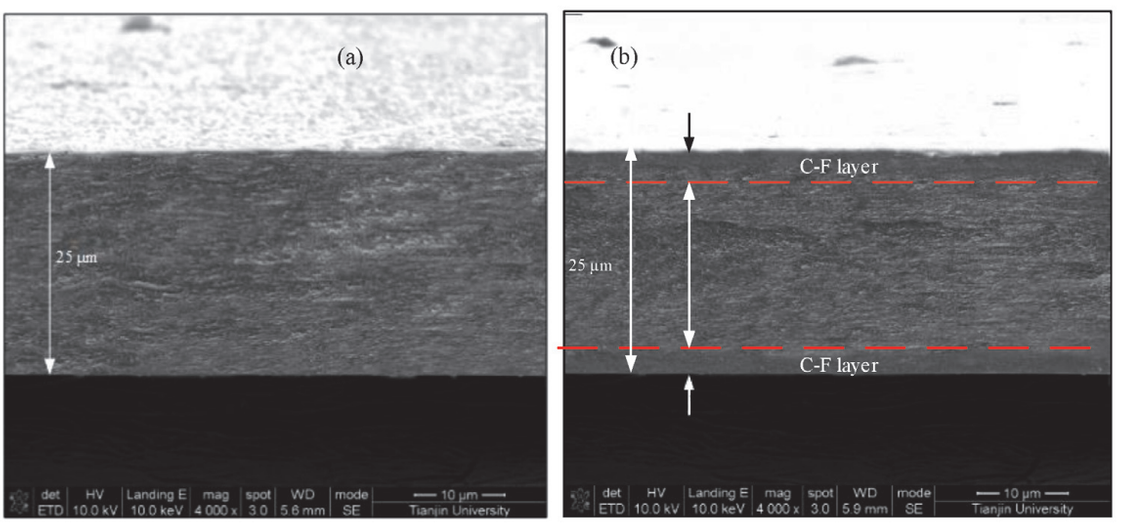

Figure 3.
The SEM of (a) original film and (b) fluorinated film of PI.

Figure 3 describes the microstructure of original PI film without fluorination and the fluorination film for 60 min by the SEM, respectively. As can be seen from the figure, a dense fluorinated layer is formed on the surface of the sample. The thickness of the sample is about 2.6 μm when the reaction time is 60 min. It is obvious that the surface molecular modification can change the chemical structure of the surface of the sample and form a C-F layer on the surface when combining infrared spectral analysis with the SEM results comprehensively.

The surface charge density of the PI sample was measured using the test system of **Figure 1(a)**. **Figure 4** shows the change of the surface charge density of the original sample and the sample fluorinated for 45 min under different corona times. It is noticeable that the surface charge density dissipates rapidly at the beginning, and then the dissipation speed gradually slows down and remains a steady trend. The positive and negative charges have similar trends. There are three main ways for surface charges to dissipate: (1) migrating to the ground electrode on the back, (2) migrating along the surface by the tangential electric field and entering the earth

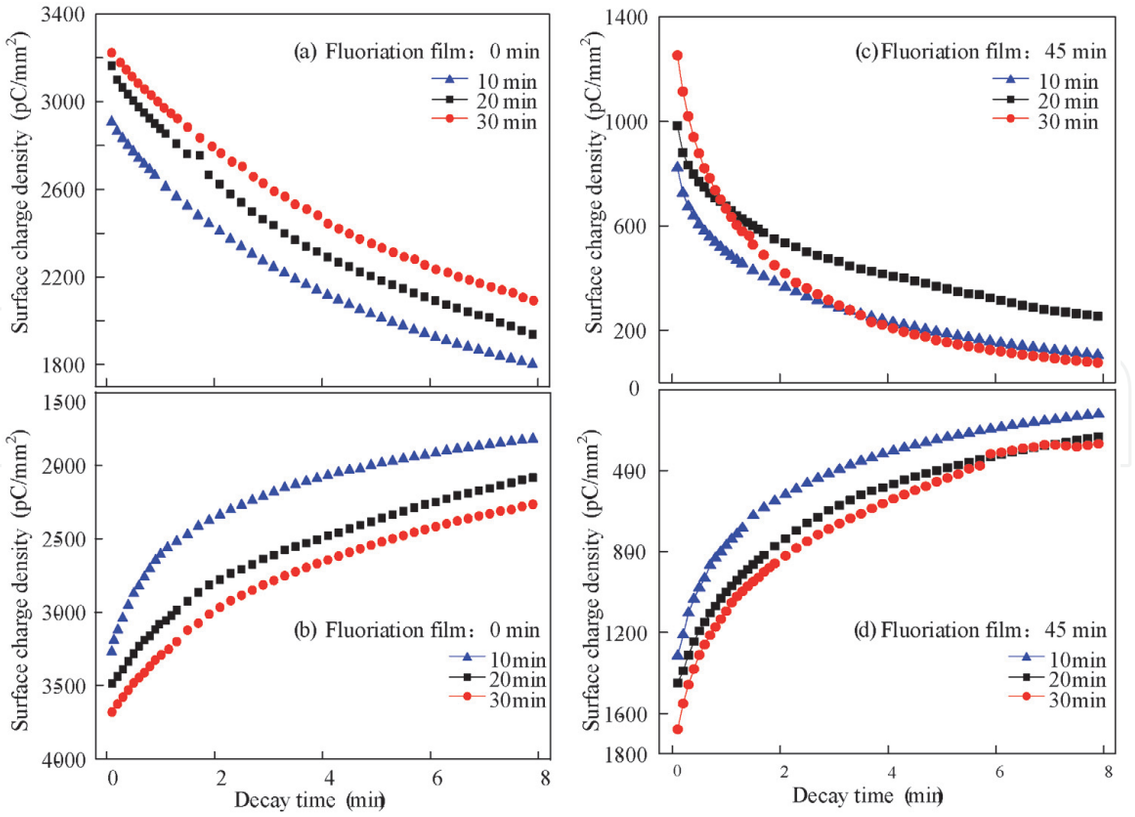

Figure 4.
The surface charge density of sample without fluorination under the (a) positive voltage, (b) negative voltage and the surface charge density of sample with fluorination under the (c) positive voltage, (d) negative voltage.

through the ground electrode, and (3) neutralizing with heterogeneous charges in the air. Which dissipating path dominates depends on various factors such as the surface characteristics of the solid medium, the gas atmosphere, and the electrode structure [17, 18]. Since the normal electric field on the film surface is much larger than the tangential electric field in this experiment. The most possible way for the surface charge to dissipate is to migrate to the ground electrode on the back and neutralize with heterogeneous charges in the air.

Figure 4(a) and **(b)** is the surface charge density of the sample without surface molecular modification. It is clear that the surface charge density gradually increases from 2900 to 3200 pC/mm^2 with the corona time rising from 10 to 30 min. During the dissipation process, the surface charge density tends to stabilize as the corona time increases, which is due to the energy required to restrain the injected charge increases with the corona time growing. The electric field formed by the charge which has been injected suppresses the large amount of the original charge transfer, alleviating the charge dissipation process [19].

According to the graph, the initial surface charge density increases with the increase of the corona time, but the dynamic of the charge is different from the dynamic of the original sample. The surface charge density of the sample under the voltage for 20 min is larger than those for 10 min and the attenuation curve is flatter, while the surface charge density of the sample under voltage for 30 min decays faster than the previous two samples. Referring to **Figure 4(c)** and **(d)**, the surface charges of the samples have the similar trend after 8 min for the samples that are under voltage for 30 and 20 min. The reason may be that the surface layer after fluorination has the fluorinated layer on the surface of the sample, which can effectively suppress the injection of charge. As the corona time increases, a large amount of charge accumulates in the fluorinated layer on the surface. When the power is turned off, the charge neutralizes and dissipates into the sample body and

the air, and most of change accumulated on the surface charge neutralizes with opposite charge in the air. Therefore, although the initial surface charge density increases when the voltage time is 30 min, most of change accumulates on the surface fluorinated layer and does not enter the deep traps inside sample, which lead to the similar trend after 8 min.

The influence of different fluorination times on the surface charge dissipation of the sample was evaluated by the dissipation time. The dissipation time is regarded as the time from the charge starting dissipates to the remaining 10% of the premier surface charge. The longer time stands for the more slowly charge dissipation. **Figure 5** shows the surface charge dissipation time under different conditions. **Figure 5(a)** is the dissipation time of the sample fluorinated 30 min under different corona times, and **Figure 5(b)** is the dissipation time of sample with fluorination time when the corona time is 10 min.

From **Figure 5(a)**, the dissipation time gradually increases as the corona time increases, and the dissipation time of the negative charge is shorter than that of the positive charge.

According to **Figure 5(b)**, the positive charge dissipation time of original sample is 80 min, whereas the negative charge is 100 min, both which are more than 1 h. After fluorination, the total dissipation time is less than 18 min, and the charge dissipation time of the sample fluorinated for 45 min is the shortest. For the original sample, the dissipation time of the negative charge is longer than the positive charge. However, the dissipation time of the negative charge of the sample after fluorination is lower than the positive charge, due to the strong electronegativity of fluorine element which can absorb electrons to form a shielding layer on the surface layer under the negative corona, thereby improving the dissipating speed.

This section uses polymer trap theory to further study the surface charge transport mechanism of polyimide materials. According to the trap theory, the trap energy level and density in the polymer can be calculated by the following formula (2) and (3).

$$\Delta E = kT \ln(\nu t) \tag{2}$$

$$N(E) = \frac{4\varepsilon_0 \varepsilon_r}{qLkTL} \frac{tdV}{dt} \tag{3}$$

ΔE is the trap energy level, T is the absolute temperature, k is the Boltzmann constant, t is the time, $N(E)$ is the trap density, L is the sample thickness, ν is the escape frequency, q is the basic charge, and V is the surface potential.

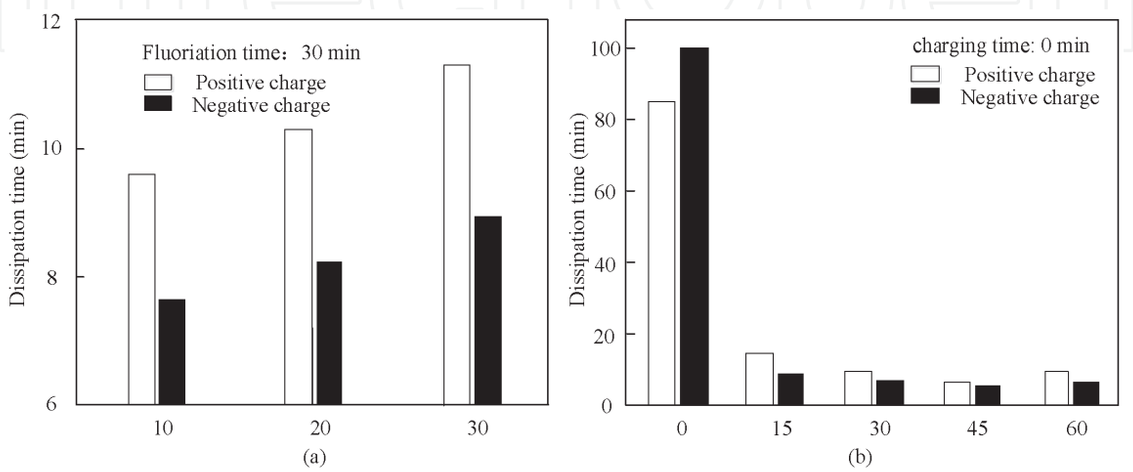

Figure 5.
The surface charge density of sample without fluorination under the (a) positive voltage and (b) negative voltage.

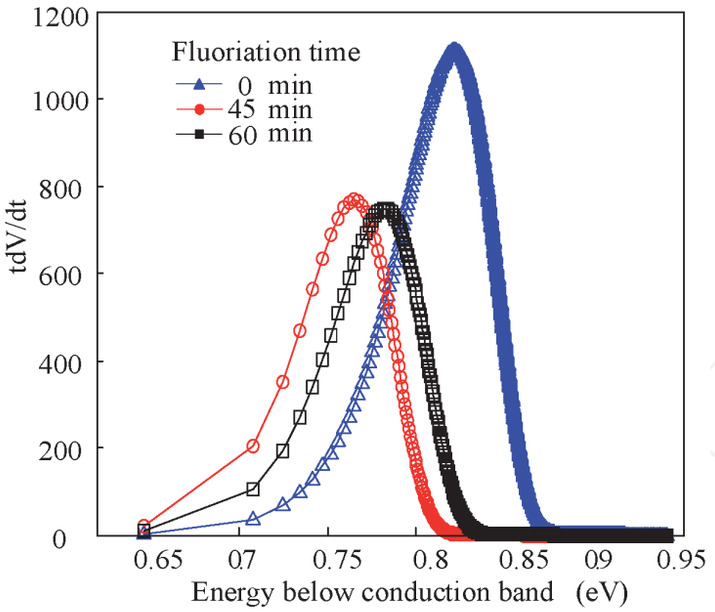

Figure 6.
The trap distributions of sample under various fluorination times.

The trap parameters of the polyimide film under different fluorination times are calculated. As shown in **Figure 6**, the energy level represents the depth of the trap. For the sample without fluorination, the trap level is most distributed at 0.84 eV, while the samples fluorinated for 45 and 60 min are most distributed at 0.76 and 0.79 eV. The results indicate that the trap level of sample with fluorination was shallower than original sample. The polyimide after fluorination makes up for some defects on the surface of the sample, thereby reducing the trap depth of the sample and causing surface charge difficult to accumulate, and dissipates faster, which is in line with the former conclusion.

3.2 The effect of molecular structure on surface charge dynamics of PI nanocomposites

Figure 7 is the SEM of the PI nanocomposite film doping with 3 and 5 wt% of Al_2O_3. The nanoparticles are dispersed in the PI matrix uniform when the mass fraction is 3 wt%, but large-size agglomerates appear with a particle size above

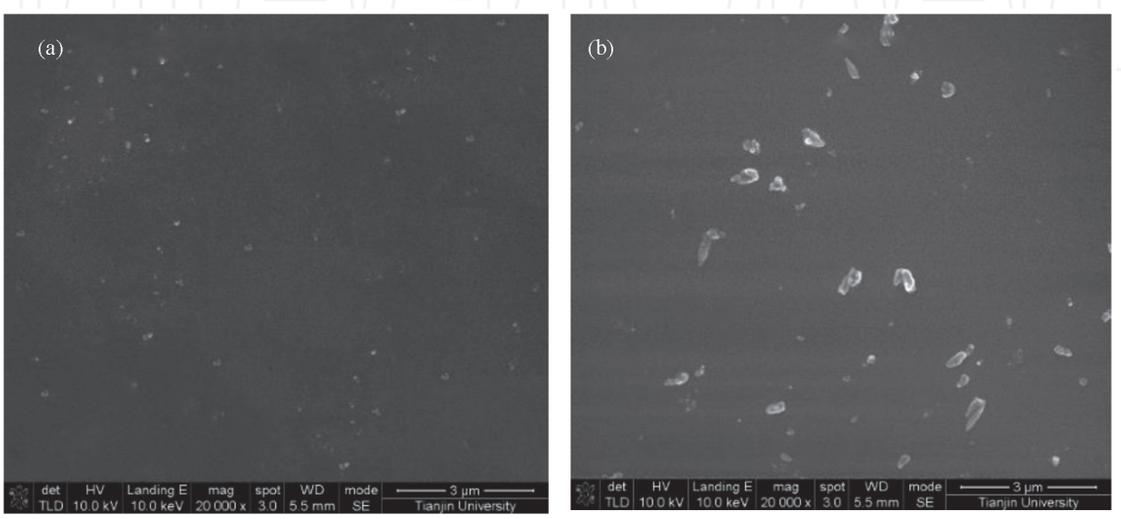

Figure 7.
The SEM images of PI films doping with (a) 3 wt% and (b) 5 wt% of Al_2O_3.

500 nm when the mass fraction is 5 wt%. Nano-composite PI films with different mass amounts are divided into two groups, one of which is subjected to fluorinate for 30 min and the other is original films.

The experiment used the surface charge dynamic measurement system to study surface charge dynamics. The conditions were to maintain relative humidity at ~40%, room temperature, grid voltages to ±3 kV, and corona times to 5, 10, and 15 min. The result is shown in **Figure 8**.

According to **Figure 8(a)**, the surface charge density gradually increases as the corona time increases, and the initial surface charge density of the negative charge is higher than the positive charge. Comparing **Figure 8(a)** and **(c)**, it is found that the surface charge density of the sample after fluorination decreased more and dissipate faster. Referring to **Figure 8**, it can be found that the fluorination has stronger effect on the PI film than the nanocomposite PI film. Comparing **Figure 8 (c)** and **(d)** with **Figure 4(c)** and **(d)**, the surface charge density of the sample with nanoparticles is higher than sample without nanoparticles and the charge dissipation is slower. The surface charge density of fluorinated PI film with Al_2O_3 decays below ±200 pC/mm^2 in a short time. But after the Al_2O_3 are added, the sample charge density is 300 pC/mm^2 after 35 min, which indicates that the sample with nanoparticles has a stronger ability to capture surface charges. These studies show that nanoparticles and surface molecular modification have opposite effect on the surface charge dynamics of polyimide films. The latter can make sample traps shallower and the former makes the surface charge agglomerate and dissipate slowly.

Figure 9 describes the surface charge dissipation of the nano-composite PI film. It is clear that the surface charge dissipating time of the fluorinated sample is

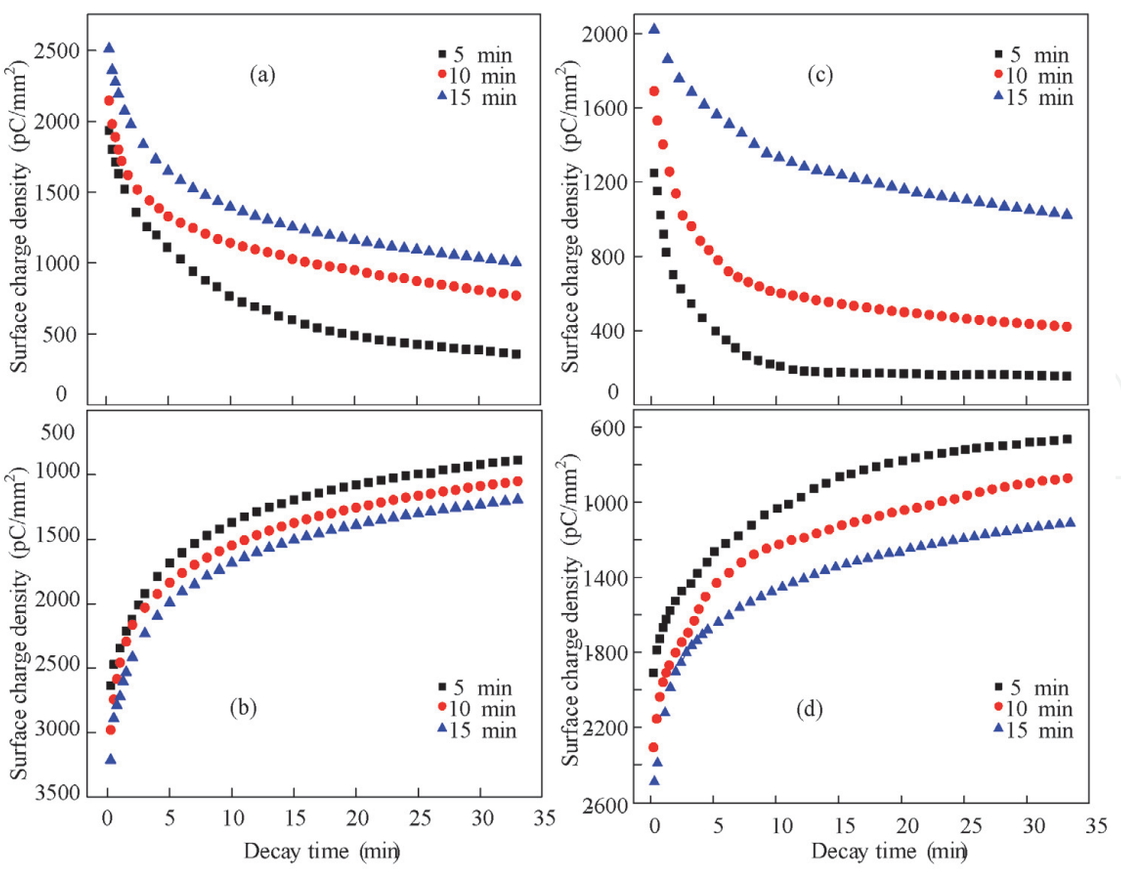

Figure 8.
The surface charge density of original sample doping with 3 wt% Al_2O_3 under the (a) positive voltage, (b) negative voltage and the surface charge density of fluorination sample doping with 3 wt% Al_2O_3 under the (c) positive voltage, (d) negative voltage.

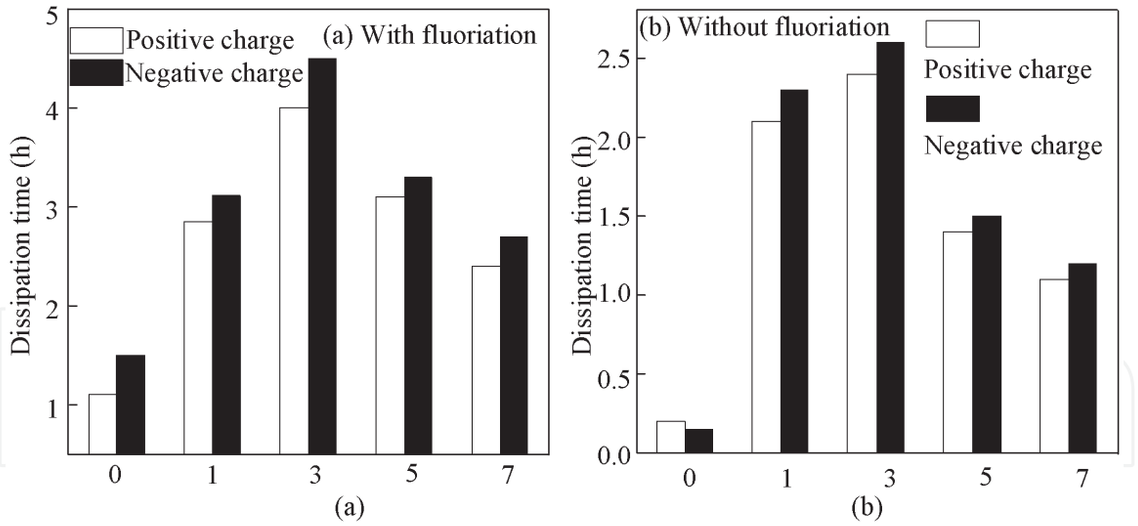

Figure 9.
The surface charge dissipation time of the nano-composite PI film (a) with fluorination (wt%) and (b) without fluorination (wt%).

shorter than the sample without fluorination, indicating that fluorination improves the surface charge dissipation. The dissipation time increases firstly and then decreases with the increase of the Al_2O_3 content for all samples. The surface charge dissipates slowly when Al_2O_3 content is 3 wt%.

In order to further study the effect of nanoparticles on the transport mechanism of the surface charge of the PI film, the trap properties are analyzed. It can be seen from **Figure 10(a)** that the nano-composite film with 3 wt% Al_2O_3 has the highest trap energy level and the most trap density, the trap energy level of the film without nanoparticles is the lowest. The trap energy level is lower when the Al_2O_3 content is 7 wt% than 3 wt%. This indicates that the interface which formed between the nanoparticles and matrix makes the trap level of nanocomposite PI deeper, and the deep trap inhibits the injection of the charge. As the content of Al_2O_3 changes, the distribution and quantity of the interface will change. When the content is high, the agglomeration will occur and affect trap depth of the sample and the accumulation as well as dissipation characteristics. This is also the reason why the dissipation time is longest when the content is 3 wt%. This chapter finds that the nanoparticles will deepen the traps of the polyimide film, increase the ability of surface charges to accumulate on the surface, and suppress the dissipation.

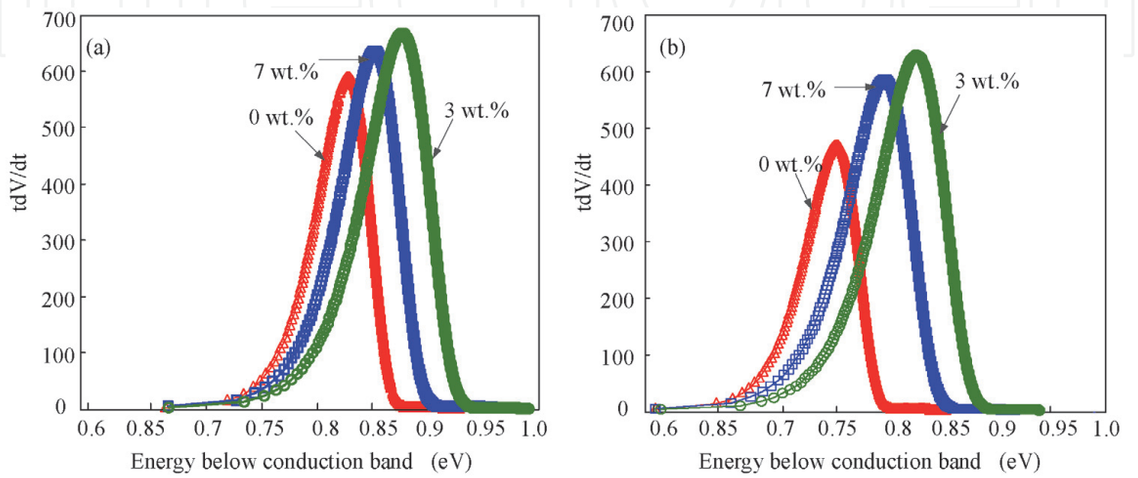

Figure 10.
The trap distributions of sample doping with various mass contents of Al_2O_3 (a) without fluorination, (b) with fluorination.

Combining the conclusion of fluorination with nanocomposites, it is clear that comprehensive application of surface molecular structure modification and nanoparticles can improve the electrical resistance while improving its surface charge dissipation, optimizing the trap distribution of the sample, and reducing the surface energy.

3.3 The effect of surface molecular modification on space charge characteristics of multilayer PI films

The samples used in the section are multilayer PI films without nanoparticles and fluorinated for 15, 30, 45, and 60 min, respectively, which are named as PI15, PI30, PI45, and PI60. In addition, the samples without fluorination named PI10 are

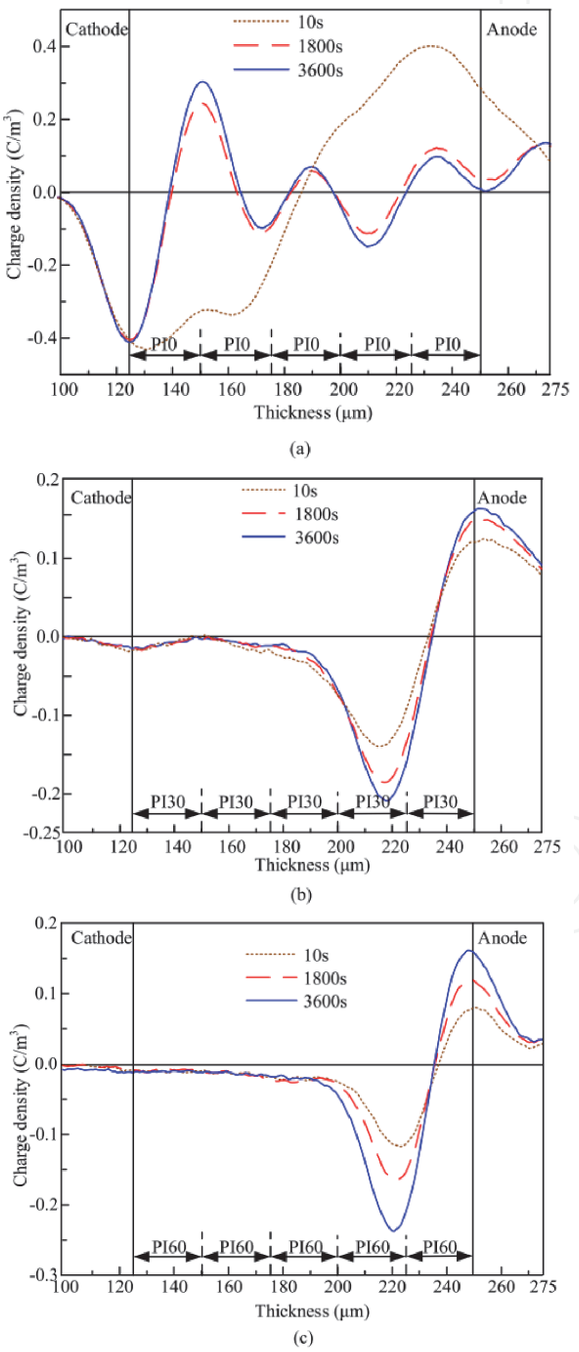

Figure 11.
The space charge distribution of multilayered PI films by stacking (a) five samples without fluorination, (b) five samples fluorinated for 30 min, (c) five samples fluorinated for 60 min.

used as the contrast group. The testing system is the PEA method in **Figure 1(b)**. During the measurement, five samples with the same fluorination time were stacked into single multilayer film, and the silicone oil was applied between the interfaces to remove air. The applied voltage time was 3600 s, and the amplitude was 5 kV.

The space charge distribution of multilayered PI films is shown in **Figure 11**. In the figure, the thickness of each layer is 25 μm. Each layer of the sample is marked with PI0, PI30, and PI60. It can be seen from **Figure 11(a)** that when the voltage time is 10 s, a certain number of homosexual charges appear near the anode and cathode. As the voltage time increases, the space charge distribution changes. When the voltage time is 1800 and 3600 s, a lot of positive charge occur near cathode, followed by the negative charge accumulating near the next interface, and then the

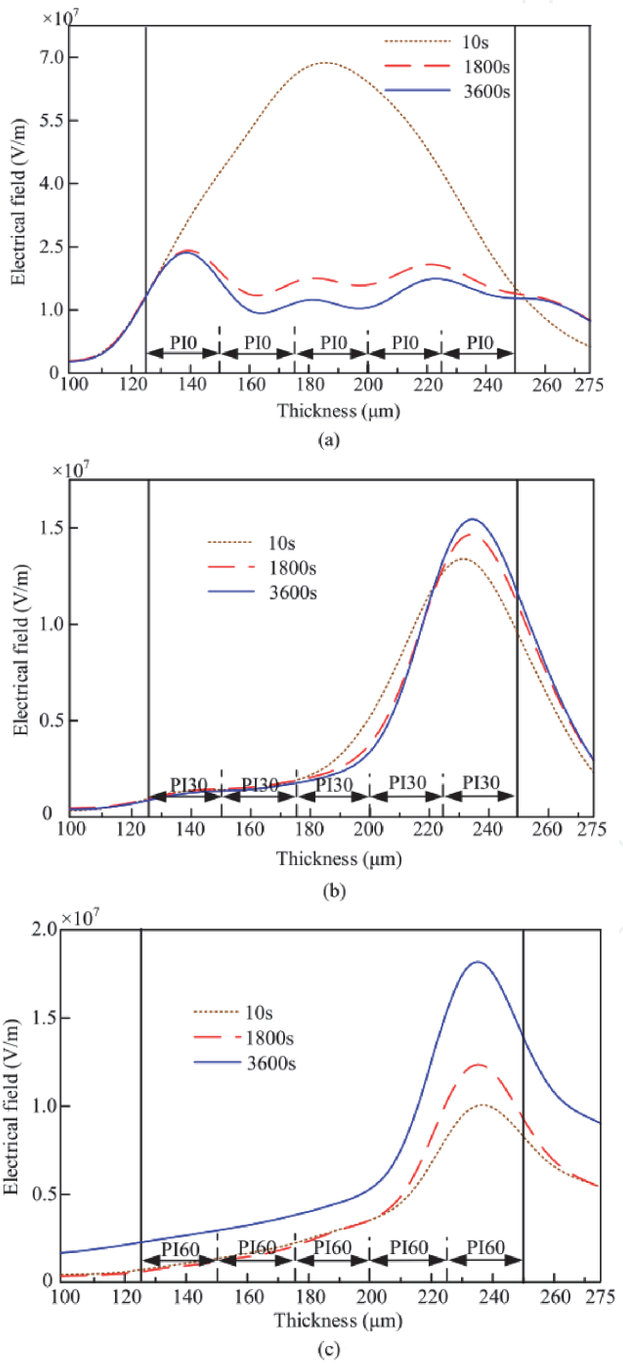

Figure 12.
The electrical distribution of multilayered PI films by stacking (a) five sample without fluorination, (b) five sample with fluorinated for 30 min, and (c) five sample with fluorinated for 60 min.

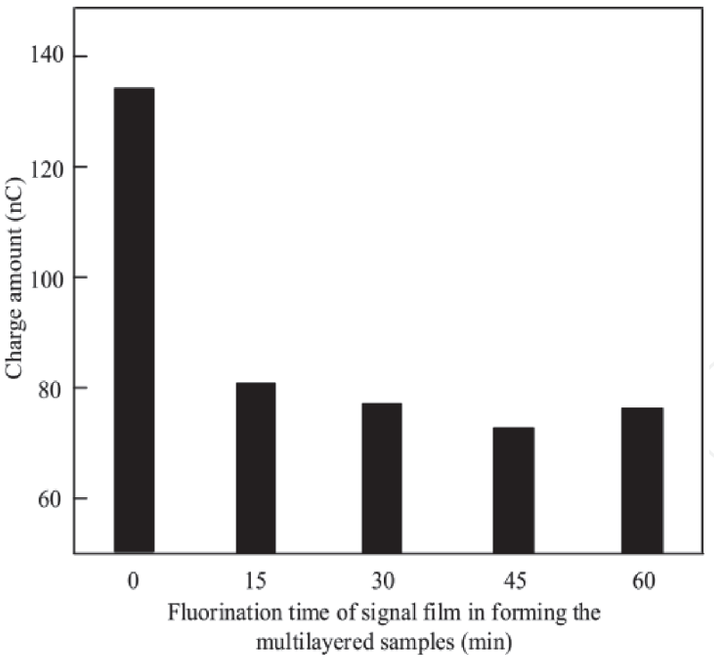

Figure 13.
Relationship between the charge of multilayer samples and the fluorination time.

positive and negative charges alternately appear, until the small amount of positive charge exists near the anode. The largest space charge density amplitude near the cathode is 0.3 C/m^3.

According to **Figure 11(b)**, the charge distribution is very different from the space charge distribution of the untreated samples. The space charge distribution of the five layers of PI30 has the same trend from 10 to 3600 s. A certain amount of positive charge accumulates near the anode, and a large amount of negative charge accumulates at 210–220 μm near the interface near the anode. The maximum space charge density amplitude is 0.21 C/m^3. In **Figure 11(c)**, the space charge distribution trend of the five-layer PI60 sample is similar with the five-layer PI30 film. In addition, the space charge distribution of the five-layer PI15 and PI45 samples has the similar trend with five-layer PI30 and PI60 samples. To avoid repetition, the space charge distribution of the two is not given in this chapter.

Figure 12 shows the distribution of the electric field of the sample after different fluorination times. In **Figure 12(a)**, the sample accumulates a large number of homosexual charges near the cathode and anode during the initial stage of applying voltage, resulting in the high electric field strength with 7.0×10^7 V/m. As the voltage time increases, the charge is transferred and accumulated inside the sample, leading to the change of electrical distribution. **Figure 11(b)** and **(c)** shows the internal electric field strength of the five-layer PI30 and PI60 samples. It can be found that the electric field strength of PI30 is much lower than PI10, which means surface molecular modification can optimize the electric field. The highest internal electric field strength of PI30 is 1.6×10^7 V/m, and PI60 is 1.8×10^7 V/m.

The studies in **Figures 11** and **12** show that the surface structure and internal trap energy level of the sample after surface molecular modification is adjusted can make the sample effectively inhibit the injection of charge into the sample, thereby suppressing the space charge accumulation in the sample.

In order to analyze the amount of space charge injected into the internal of sample, the total amount is calculated according to formula (4):

$$Q = \int_{d_2}^{d_1} \left| \rho(x) \right| S \mathrm{d}x \tag{4}$$

In the formula, S is the effective area, and d_1 and d_2 are the thickness start and end positions of the sample. $\rho(x)$ is the charge density at x.

The charge amount of the sample with different fluorination times is shown in **Figure 13**. It can be seen that the sample without fluorination has a charge of 135 nC, and the amount of space charge of all sample with fluorination is below 80 nC. With the increase of the fluorination time, the amount of charge decreases slightly and then increases again. The charge amount of sample fluorinated for 45 min is the lowest (75 nC) among all the fluorinated samples.

4. Conclusions

In this chapter, nano-composite polyimide films with different amounts of Al_2O_3 are prepared by in-situ polymerization. PI films with and without surface molecular modification are prepared. Based on the DC corona method and PEA method, the surface charge and space charge dynamic of the sample were analyzed. The main research results obtained are as follows:

1. The infrared spectroscopy and SEM images show that surface molecular modification can effectively change the chemical structure of the sample surface and form a dense CF layer on the surface. The surface charge test shows that the number of shallow traps on the surface of the PI film after surface molecular modification increases, making it difficult to accumulate charges on the surface and improving charge dissipation, which can effectively solve the problem of surface charge accumulation for polymer. And in this chapter, the PI films fluorinated for 45 min has the lowest trap energy level and the lest charge accumulation.

2. For nano-composite PI film, the nanoparticles increase the surface trap level and density of the PI film, generating charge accumulation and block the charge dissipation. The dissipation time of films increases first and then decreases with Al_2O_3 content increases. The PI film doping with 3 wt% Al_2O_3 has the highest trap energy level and the largest trap density, which brings the most serious charge accumulation and the longest dissipation time.

3. The amount of space charge of the multilayer PI film decreased from 135 75 nC with the time of surface molecular modification rising from 0 to 45 min, but the amount of charge decreases slightly when the time increases from 45 to 60 min.

4. This chapter finds that the comprehensive application of the surface molecular modification and nanoparticles can effectively improve the polyimide's electrical properties, regulating its surface charge distribution and the trap level of the sample.

DOI: http://dx.doi.org/10.5772/intechopen.92024

Author details

Boxue Du, Ranran Xu, Jiwen Xing and Jin Li*
Key Laboratory of Smart Grid of Education Ministry, School of Electrical and Information Engineering, Tianjin University, Tianjin, China

*Address all correspondence to: lijin@tju.edu.cn

References

[1] Kirkici H, Serkan M, Koppisetty K. Nano/micro dielectric surface flashover in partial vacuum. IEEE Transactions on Dielectrics and Electrical Insulation (TDEI). 2007;**14**(4):790-795

[2] Maity P, Basu S, Parameswaran V, et al. Degradation of polymer dielectrics with nanometric metal-oxide fillers due to surface discharges. IEEE Transactions on Dielectrics and Electrical Insulation (TDEI). 2008;**15**(1):52-62

[3] Bin M, Gubanski SM, et al. Dielectric properties and resistance to corona and ozone of epoxy compositions filled with micro-and nano-fillers. Annual Report Conference on Electrical Insulation and Dielectric Phenomena; 2009. pp. 672-677

[4] Venkatesulu B, Joy Thomas M. Corona aging studies on silicone rubber nanocomposites. IEEE Transactions on Dielectrics and Electrical Insulation (TDEI). 2010;**17**(2):625-634

[5] Venkatesulu B, Joy Thomas M. Erosion resistance of alumina-filled silicone rubber nanocomposites. IEEE Transactions on Dielectrics and Electrical Insulation (TDEI). 2010;**17** (2):615-624

[6] Iyer G, Gorur RS, Krivda A. Corona resistance of epoxy nanocomposites: Experimental results and modeling. IEEE Transactions on Dielectrics and Electrical Insulation (TDEI). 2012;**19**(1): 118-125

[7] Du BX, Zhang JW, Liu Y. Effect of concentration on tracking failure of epoxy/TiO2 nanocomposites under dc voltage. IEEE Transactions on Dielectrics and Electrical Insulation (TDEI). 2012;**19**(5):1750-1759

[8] Tanaka T, Mulhaupt GCMR. Polymer nanocomposites as dielectrics and electrical insulation-perspectives for processing technologies, material characterization and future applications. IEEE Transactions on Dielectrics and Electrical Insulation (TDEI). 2004;**11** (5):763-784

[9] Kharitonov AP. Direct fluorination of polymers-from fundamental research to industrial applications. Progress in Organic Coating. 2008;**61**:192-204

[10] Tressaud A, Durand E, Labrugere C, et al. Modification of surface properties of Carbonbased and polymeric materials through fluorination routes: From fundamental research to industrial applications. Journal of Fluorine Chemistry. 2007;**128**:378-391

[11] Zhong JH. Research on Corona resistance of hybrid polyimide film. Engineering Plastic. 2005;**33**(9):13-15

[12] Junwei Z. Insulation characteristics of PI/ZnO corona-resistant hybrid film. Chinese Society for Electrical Engineering. 2009;**29**(34):122-127

[13] Hongyan L. Dielectric properties of polyimide/Al_2O_3 composite film. Chinese Society for Electrical Engineering. 2006;**26**(20):166-169

[14] Jiang Y, An Z, Liu C, et al. Influence of oxyfluorination time on space charge behavior in polyethylene. IEEE Transactions on Dielectrics and Electrical Insulation (TDEI). 2010;**17** (6):1814-1823

[15] Kharitonov AP, Kharitonova LN. Surface modification of polymers by direct fluorination: A convenient approach to improve commercial properties of polymeric articles. Pure and Applied Chemistry. 2009;**81**: 451-471

[16] Hosono T, Kato K, Morita A, et al. Surface charges on alumina in vacuum with varying surface roughness and

electric field distribution. IEEE Transactions on Dielectrics and Electrical Insulation (TDEI). 2007;**14** (3):627-633

[17] Das-Gupta DK. Electrical properties of surfaces of polymeric insulators. IEEE Transactions on Dielectrics and Electrical Insulation. 1992;**27**(5):909-923

[18] Fu M, Chen G, Dissado L, et al. The effect of gamma irradiation on space charge behaviour and dielectric spectroscopy of low-density polyethylene. In: International Conference on Solid Dielectrics; 2007. pp. 442-445

[19] Wang FP, Xia ZF, Qiu XL, et al. Piezoelectric properties and charge dynamics in poly(vinylidene fluoride-hexafluoropropylene) copolymer films with different content of HFP. IEEE Transactions on Dielectrics and Electrical Insulation (TDEI). 2006;**13** (5):1132-1139